Simulation of Large-Eddy Structures in a Turbulent Boundary Layer

Mohamed Gad-el-Hak*
University of Notre Dame, Notre Dame, Indiana
and
Ron F. Blackwelder†
University of Southern California, Los Angeles, California

An active flow control device to generate large-scale, periodic structures in a turbulent shear flow is developed. A flat plate towed in a water channel is used as a test bed. A cyclic jet issuing from a spanwise slot is used to collect the turbulent boundary layer for a finite time during its "on" period. When the jet is turned "off," all of the turbulent fluid is released instantaneously in one large eddy that convects downstream. Flow visualization and hot-film probe measurements are used together with the VITA pattern recognition algorithm to demonstrate the viability of the flow control method. The instantaneous velocity signal is used to compute important statistical quantities of the random velocity field, such as the mean, the root mean square, the spectral distribution, and the probability density function. When optimized for a given boundary layer, the cyclic jet produces periodic structures that are qualitatively similar to the random, naturally occurring ones. These structures seem to trigger the onset of bursting events near the wall. Thus, the present device generates periodic structures in both the outer and inner regions of a turbulent boundary layer.

Nomenclature

D	= size of region to be protected from normal boundary-layer fluctuations
d	= streamwise width of the injection slot
dU_j/dt	= rate of change of injection velocity
f	= perturbation frequency
L	= distance downstream of injection slot
P	= period of cyclical jet
$P(U)$	= probability density function of the streamwise velocity
$R(\tau)$	= autocorrelation coefficient
R_{δ^*}	= displacement thickness Reynolds number, $U_\infty \delta^*/\nu$
R_θ	= momentum thickness Reynolds number, $U_\infty \theta/\nu$
$S(f)$	= normalized power spectral density
$S'(f)$	= dimensional power spectral density, $\overline{u^2}\, S(f)$
t	= time
$U_{j\max}$	= maximum jet velocity
$U(t)$	= instantaneous streamwise velocity
$U_j(t)$	= instantaneous injection speed
U_∞	= towing speed
$\overline{U}$	= mean longitudinal velocity
$u(t)$	= streamwise velocity fluctuations, $U(t) - \overline{U}$
u_τ	= friction speed
$\overline{u^2}$	= mean square of longtudinal velocity fluctuations
W	= spanwise width of injection slot
x,y,z	= Cartesian coordinates fixed with the plate
y^+	= height above plate in wall units, $y\, u_\tau/\nu$
δ	= boundary-layer thickness
δ^*	= displacement thickness
Θ	= angle of injection with respect to freestream direction
θ	= momentum thickness
ν	= kinematic viscosity
τ	= correlation time interval

Received July 28, 1986; revision received Dec. 10, 1986; presented as Paper 87-0587 at the AIAA 25th Aerospace Sciences Meeting Reno, NV, Jan. 12-15, 1987.

*Professor of Aerospace and Mechanical Engineering. Member AIAA.

†Professor of Aerospace Engineering. Member AIAA.

I. Introduction

TURBULENT boundary layers occur on bodies moving relative to a fluid at high Reynolds numbers. The turbulent layer is known to consist of large, three-dimensional eddy structures that scale with the boundary thickness, δ, and extend across the entire layer. These eddies control the dynamics of the boundary layer in the outer region, such as entrainment, turbulent production, etc. The large eddies appear randomly in space and time and hence it is difficult to predict when an eddy will be present at a specific location and time. However, in some applications it may be desirable to know if and when such large eddies will arrive at a given location. For example, provided that the large-eddy structures are periodic, adaptive optics may be used on airborne laser platforms to reduce or eliminate optical distortion caused by the turbulence in the aircraft's boundary layer.

The present investigation is aimed at exploring the feasibility of generating large-scale, periodic structures in a highly turbulent flowfield. The active flow control method used in this investigation is a cyclic, two-dimensional jet issuing from the wall of a boundary layer to collect the turbulence for a finite time and then release the collected fluid instantaneously in one large eddy that convects downstream once every period.

The concept of large-eddy generation is detailed in Sec II. Description of the experimental setup is given in Sec. III. Sections IV through VIII contain the results of the flow visualization and fast-response velocity-probe measurements conducted to demonstrate the concept of artificial generation of large eddies in a turbulent boundary layer. Finally, a brief summary is presented in Sec. IX.

II. Large-Eddy Generating Device

A large-eddy generating device is sought for altering the eddy structure in an existing turbulent boundary layer. In principle, the device should collect the turbulent fluid within the boundary layer for a finite time period and then release it instantaneously in one large eddy to pass downstream. Thus, during the collection period, the flow downstream of the device would be relatively free of the existing turbulence. This period would be followed by the passage of one large eddy, and the cycle would then repeat itself.

One practical means of realizing the above idealized concept is to use a small, two-dimensional, cyclic jet as shown in Fig. 1 and discussed in detail in Sec. III C. As the fluid issues from the jet, the existing boundary layer will be entrapped and form a large eddy. Meanwhile, downstream a thinner boundary layer must result since it is deprived of much of its turbulence. In the early stages of the cycle, the jet velocity should increase at a sufficient rate to contain most of the turbulence. Eventually, a point is reached where no further velocity increase is possible for a given power level. The jet could be shut off immediately and the collected turbulence would be swept downstream as one large eddy and the cycle would begin again. Consequently, the protected area of size D downstream would have a very thin layer over it during most of the period, followed by the passage of one large eddy which appears periodically. This method could be further enhanced by using suction over part or all of the distance L in Fig. 1. When phase-locked with the pulsating jet, the suction could further reduce or eliminate the thin boundary layer during the period that the turbulence is being collected upstream by the jet.

Techniques similar to the method described above have been successfully used for generating and/or controlling the large eddies in turbulent boundary layers. Viets[1] used an asymmetrical rotating cam embedded in the wall to produce large eddies in boundary layers with zero and adverse-pressure gradients. By using this device in a wide-angle diffuser, Viets et al.[2] were able to decrease the natural separation and improve the diffuser's performance. Alternatively, thin ribbons could be placed in the boundary layer to act as large-eddy breakup devices. Bushnell[3] and Anders and Watson[4] have shown that, at zero angle of attack, two thin ribbons, one placed above a flat plate and one parallel to it, lead to a reduction in the skin friction of the boundary layer. Oscillating these devices could produce a series of large and smaller eddies in the boundary layer. However, it is felt that the pulsating jet has greater practical advantage because it is easier to control and has no external moving parts. In addition, by properly synchronizing the jet's amplitude, angle and acceleration, a greater degree of controllability would appear to be achievable with the proposed jet. Similar developmental research by Gad-el-Hak and Blackwelder[5,6] has led to a pulsating jet device that controls the formation and growth of the large-bound vortices on delta wings and similar lifting surfaces.

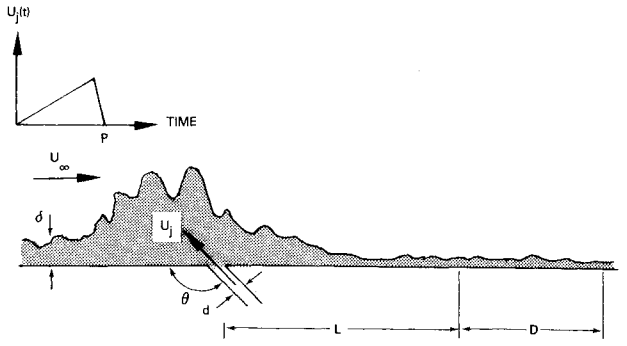

Fig. 1 Large-eddy generating device consisting of an oscillating jet of fluid which periodically blocks the normal passage of the turbulent boundary layer.

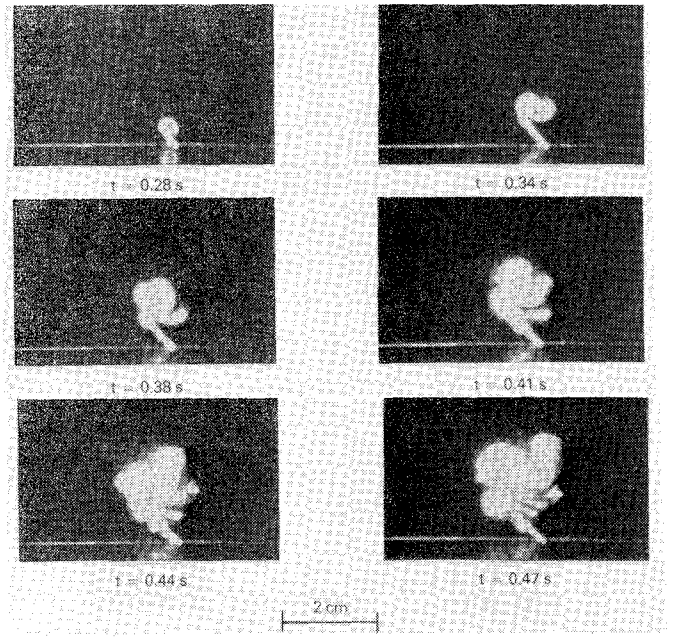

Fig. 2 Periodic injection from spanwise slot. Flat plate is stationary and maximum injection speed = 45 cm/s.

III. Experimental Approach

A. Towing Tank

Turbulent and laminar boundary layers were generated by towing a flat plate in a water channel that is 18-m long, 1.2-m wide, and 0.9-m deep. (The towing tank has been described by Gad-el-Hak et al.[7]) The flat plate was rigidly mounted under a carriage that rides on two tracks mounted on top of the tank. During towing, the carriage was supported by an oil film to ensure a vibrationless tow, having an equivalent freestream turbulence of about 0.1%. The carriage was towed by two cables driven through a reduction gear by a 1.5-hp Boston Ratiotrol motor. The towing speed was regulated within an accuracy of 0.1%. The system was able to achieve towing speeds between 5 and 150 cm/s for the present study, however, all of the runs reported here were conducted at a speed of 20 cm/s.

B. Flat Plate

A unique, zero-pressure-gradient flat plate was constructed for the present investigation. The 1×2 m structure was made of glass-reinforced polycarbonate plate 6 mm thick, glued to a stainless-steel frame designed for minimum obstruction to the flow. The plate had an elliptic nose at the leading edge and an adjustable lifting flap at the trailing edge. To avoid leading-edge separation and premature transition, the flap was adjusted so that the stagnation line near the leading edge was located on the working surface of the plate. The plate was smooth and flat to within a few micrometers making it an ideal test bed for boundary-layer research. A laminar boundary layer was obtained over the entire working surface for towing speeds in the range of 5-80 cm/s. Trips were used to generate a fully developed turbulent boundary layer. The trips were brass cylinders 0.32 cm in diameter and 0.25-cm high placed 5 cm downstream of the leading edge with their axes perpendicular to the flat plate.

C. Large-Eddy Generating Device

The large-eddy generating device, shown schematically in Fig. 1, consisted of a two-dimensional, spanwise, cyclic jet. As mentioned in Sec. II, the periodic jet was used to collect the turbulent boundary layer for a finite time and then release all of the flow instantaneously in one large eddy that convects

downstream. The primary parameters of this jet are its physical size d and W, amplitude of velocity U_j, frequency f, angle Θ, and acceleration of jet velocity dU_j/dt. The width of the jet d is dictated by the boundary-layer thickness, i.e., the jet must be smaller than the boundary thickness δ. Its spanwise width W is dictated by the width of the protected area and is typically several boundary-layer thicknesses. In the present experiment, d was 1 mm and W was 150 mm. The two-dimensional jet was located 62 cm from the leading edge where the boundary-layer thickness was 23 mm. The other four parameters are clearly interrelated and cannot necessarily be examined independently. Nevertheless some guidelines and ranges can be established; e.g., the frequency f of the artificial perturbation should match the mean frequency of the naturally occurring large-eddy structures. Therefore, f must be of order U_∞/δ.[8] The initial range of exploration used a velocity amplitude of the order of U_∞ and a jet frequency in the range of $0.1 \leq f\delta/U_\infty \leq 1.0$. The jet angle Θ should be greater than 90 deg as shown in Fig. 1 to maximize the containment of the boundary-layer turbulence. Several angles in this range should be explored; in the initial phase of the investigation, this angle was fixed at $\Theta = 135$ deg. The optimum acceleration (i.e., temporal variation of the jet velocity) may not necessarily be sinusoidal; consequently, forward and rearward facing ramp functions, triangular functions, etc., were explored.

The periodic jet was driven by a pressurized supply of secondary fluid. The laboratory's air supply was used to pressurize a stainless-steel tank containing water. The maximum velocity of the secondary fluid was determined by the pressure level in the reservoir and was controlled by using a pressure regulator on the air supply line. The velocity issuing from the reservoir was calibrated versus the imposed pressure using a rotameter. A ball valve driven by a stepping motor provided the temporal control of the secondary fluid's conduit. The important temporal parameters governing the jet will be denoted by (a,b,c), where a is the time required for acceleration to the maximum jet velocity, b the corresponding deceleration time to zero velocity, and c the time delay to the beginning of the next cycle. $a,b,$ and c are measured in seconds and the period of the jet perturbation is their sum. The acceleration, deceleration, and delay time of the valve were controlled within the limitations of the experimental apparatus using an APPLE II microcomputer. For example, a slow opening followed by fast closing, a symmetric cycle followed by a given delay before the starting of a new cycle, etc., were studied. The controlled secondary flow passed through a small conduit to an internal reservoir directly behind the slot that was built into the flat plate. This reservoir ensured that the ejection speed was constant within 2% along the entire spanwise slot thus providing a uniform two-dimensional jet.

D. Visualization Methods

To visualize the large eddies and near-wall events in the natural and perturbed turbulent boundary layers, different-color fluorescent dyes were used. The dyes were seeped into the boundary layer through a spanwise slot 0.15-mm wide and 15-cm long, and located 77-cm downstream of the leading edge of the flat plate. The dye slot was milled at a 45-deg angle inclined toward the plate's trailing edge to minimize the flow disturbance. Dye was also introduced through the periodic jet by mixing minute amounts of fluorescent dye with the secondary fluid in the pressure tank.

The fluorescent dyes were illuminated using a sheet of laser light projected in the desired plane. This provided an extra degree of freedom in observing the large-eddy structures and the bursting events, because both the tracer and the light location could be controlled independently within the limitations of the experimental apparatus. In order to generate a sheet of light, a 5-W argon-ion laser (Spectra Physics Model 164) was used with a mirror mounted on an optical scanner having a natural frequency of 720 Hz (General Scanning, Inc.) and driven by a sine-wave signal generator of the desired frequency. The frequency of the sine wave was usually set equal to the inverse of the shuttler speed of the camera. The light sheets were approximately 1-mm thick, which was sufficient to resolve the large structures within the turbulent regions. A vertical sheet of laser light parallel to the flow was used to visualize side views of the large-eddy structures in the x-y plane. The sheet was always projected along the centerline of the plate and jet.

E. Velocity Measurements

Miniature boundary-layer hot-film probes (TSI Model 1260) were used in the present investigation to measure the longitudinal mean and fluctuating velocities. The probe diameters were 0.025 mm, and their sensing lengths were 0.25 mm. The hot films were calibrated in the freestream at several towing speeds. A probe traverse powered by a stepping motor and controlled through an APPLE II microcomputer was used for surveying the boundary layers. Conventional statistical quantities, such as the mean, the root mean square, the spectral distribution, the autocorrelation coefficient, and the probability density function, were computed from the velocity signals.

F. Burst Detection Algorithm

The purpose of the present investigation was to determine the effectiveness of the periodic injection of secondary fluid on the large-eddy structures that dominate the outer portions of a turbulent boundary layer. However, the initial visualization experiments indicated that the artificial eddies affected the low-speed streaks and bursting events that occurred very near the wall. To further investigate this important finding, a detection algorithm was used to more objectively detect the bursts.

The burst detection algorithm employed in the present investigation was the variable-interval time-averaging (VITA) technique developed by Blackwelder and Kaplan.[9] The signal from a single hot-film probe located at $y^+ = 20$ was used for the burst detection algorithm. The program counted the number of bursts that occur near the wall and recorded their intensities.

IV. Periodic Injection in the Absence of Boundary-Layer Flow

A typical example of the ejection of water, mixed with fluorescent dye, in the absence of boundary-layer flow (the flat plate was held stationary in the water channel) is shown in the photographs in Fig. 2. A vertical sheet of laser light perpendicular to the spanwise slot illuminated the dyed fluid issuing from the slot. The flow speed increased linearly from 0–45 cm/s at an acceleration rate of 150 cm/s^2 followed by a deceleration from 45–0 cm/s at a rate of 450 cm/s^2; thus the temporal parameters were (0.3, 0.1, 0). The leading edge of the flat plate is located to the left of the side view shown in the figure, and the time in seconds measured from the starting cycle is shown under each photograph. It is clear that the secondary flow forms a clockwise-rotating vortex as it comes out of the 135-deg slot. The presence of the wall of the flat plate influenced the evolution of this vortex. The maximum injection speed, the acceleration rate, and the deceleration rate also affected the flow from the spanwise slot.

The instantaneous injection velocity of the cyclic jet can be recorded by placing a hot-film probe just outside the spanwise slot. Typical time record is shown in Fig. 3a for a periodic injection having maximum injection speed of 140 cm/s and temporal parameters of (0.3, 0.1, 0.24). The sensitive element of the hot-film probe was placed parallel to the spanwise slot at a distance of 0.5 mm ($0.5d$) from the two-dimensional orifice. The flow from the slot shown in Fig. 3a is clearly turbulent. At lower maximum injection speed, the flow is less turbulent as shown in Fig. 3b. In the latter case, the acceleration/decelera-

tion motion of the valve was symmetric and the temporal parameters were (0.04, 0.04, 0.11). It is clear from the injection cycles shown in Fig. 3 that excellent repeatability was achieved.

V. Periodic Injection into a Turbulent Boundary Layer

The mean flow parameters were measured and compared with standard boundary layers. At a freestream speed of 20 cm/s and at the two stations considered in the present investigation $x = 67$ and 100 cm, the boundary-layer thicknesses were 2.34 and 3.25 cm, the momentum thickness Reynolds numbers were $R_\theta = 455$ and 632, and the displacement thickness Reynolds numbers were $R_{\delta^*} = 585$ and 813, respectively. The mean and root-mean-square longitudinal velocity profiles of the turbulent boundary layer agreed well with those for the zero-pressure-gradient flat plate at the same Reynolds number as reported by Purtell et al.[10] The mean profiles always had a well-defined linear, logarithmic, and wake regions.

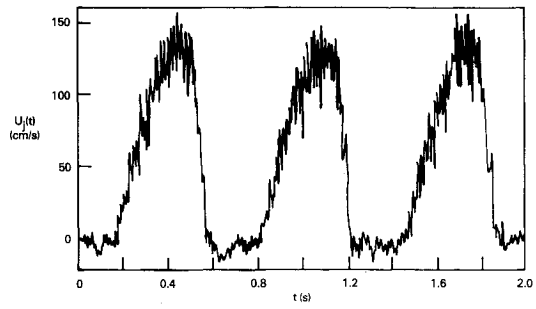

a) Maximum injection speed = 140 cm/s; acceleration for 0.3 s; deceleration for 0.1 s; time delay = 0.24 s.

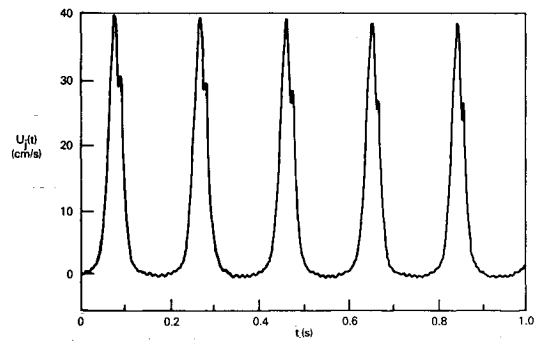

b) Maximum injection speed = 40 cm/s; acceleration and deceleration for 0.04 s; time delay = 0.11 s.

Fig. 3 Instantaneous injection velocity from spanwise slot.

In Fig. 4, the turbulent boundary-layer flow was from left to right and the secondary fluid from the slot was premixed with minute amounts of fluorescent dye. The flow was visualized just downstream of the injection slot. The temporal parameters for the periodic injection were (0.4, 0.25, 0) and the maximum injection speed was 20 cm/s. The time in seconds from the start of a typical cycle is indicated under each photograph. As shown in the figure, large-eddy-like structures are formed downstream of the spanwise slot. The shear flow in the boundary layer interacts in a unique way with the clockwise-rotating vortex issued periodically from the slot to form the structures marked by the dye. These structures stretch while convecting downstream. Two consecutive structures are separated by a distance that depends on the reduced jet frequency, $f\delta/U_\infty$, which in the present example was 0.18.

A different perspective of the flowfield is achieved by dying both the incoming turbulent boundary-layer flow as well as the cyclic, secondary fluid from the spanwise slot. In Fig. 5, the dark yellow dye (shown here as the darker shaded region) is introduced upstream of the injection slot near the leading edge of the plate, and the lighter color dye (shown here as the lighter shaded region) marks the periodic flow from the spanwise slot. The natural, random large-eddy structures are visualized in the first photograph at $t = 0$ (origin of time coincides with the start of the cyclical injection). The periodic jet introduced into the natural boundary layer had a maximum injection speed of 20 cm/s, temporal parameters of (1.0, 0.7, 0) and a reduced frequency $f\delta/U_\infty = 0.07$. At the end of the opening cycle (fourth frame in Fig. 5 at $t = 1.05$ s), the injected fluid reaches approximately the same height as that of the natural boundary layer. However, at $t = 1.45$ s (last frame in Fig. 5), the interaction between the natural and artifical eddies results in the large intrusion of the lighter dye into the potential flow region. The thickness of this region is almost twice

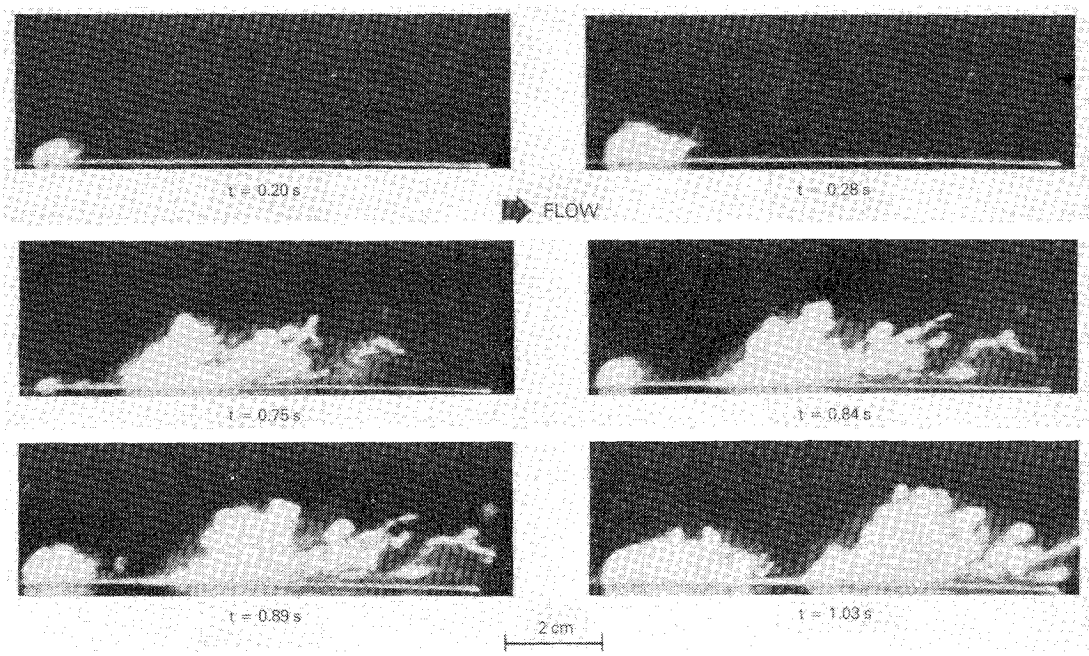

Fig. 4 Periodic injection into a turbulent boundary layer: $U_\infty = 20$ cm/s, maximum injection speed = 20 cm/s, acceleration for 0.4 s, deceleration for 0.25 s, zero delay time.

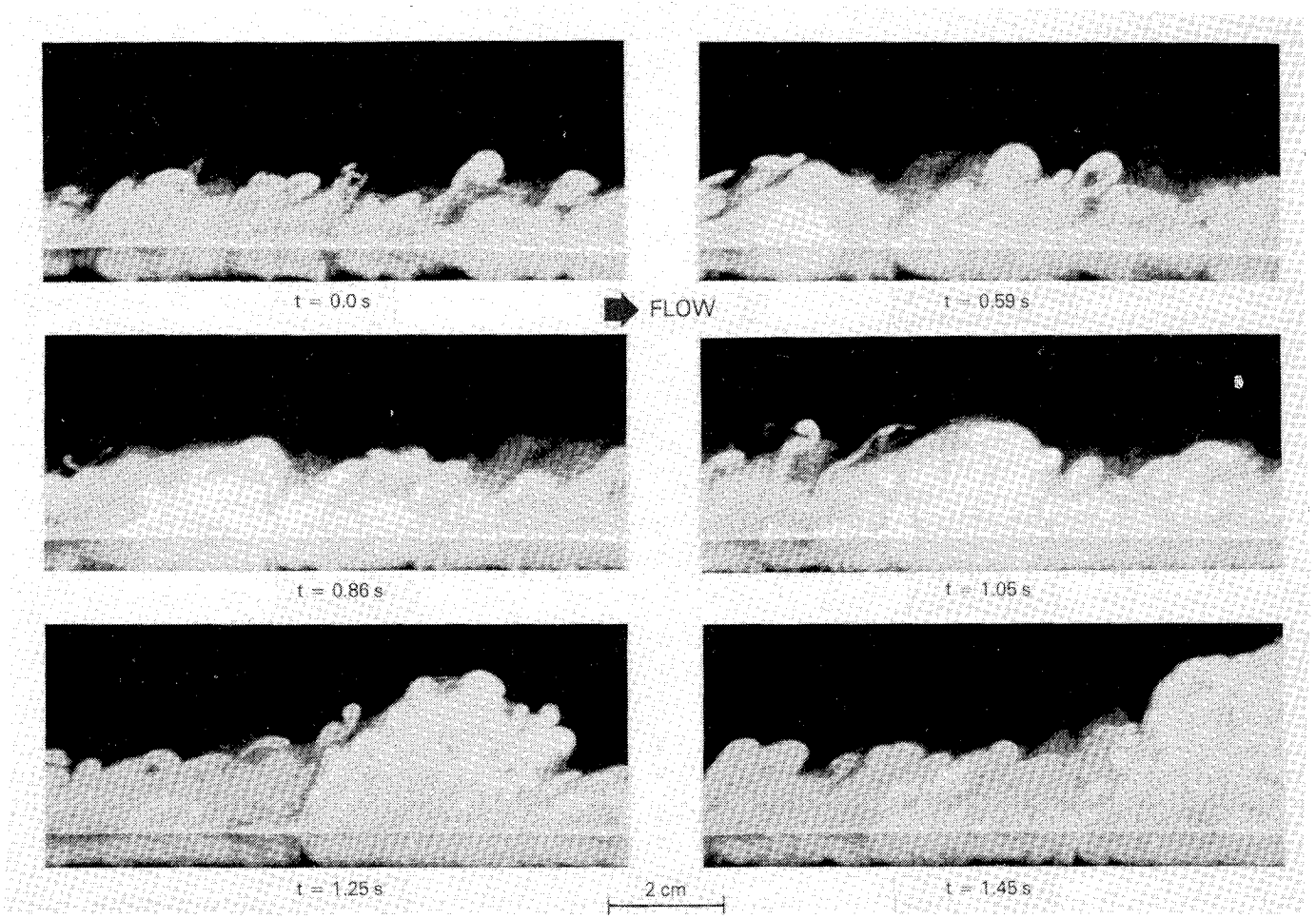

Fig. 5 Turbulent boundary layer is marked by dark yellow dye (shown here as darker shaded region). A lighter dye (shown here as lighter shaded region) marks the periodic flow from the spanwise slot. Although the initial spanwise vortex introduced into the boundary layer is relatively small, its interaction with the natural eddies results in a very large bulge.

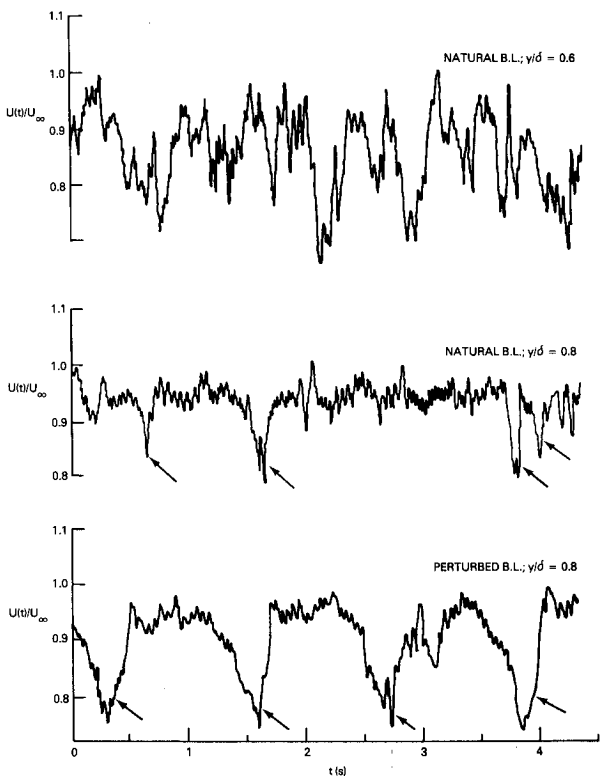

Fig. 6 Instantaneous streamwise velocity records: $U_\infty = 20$ cm/s, $x = 100$ cm.

that of the natural boundary-layer thickness. This unusual event may have been the result of a chance phasing between the perturbation and an existing eddy structure. It illustrates that under appropriate conditions, very large dynamical eddies can be obtained.

The generated eddies were most dramatically altered by varying the maximum velocity and period of the perturbation jet. With the maximum jet velocity of 20 cm/s, the resulting eddy typically had a height comparable to the normal eddies, i.e., approximately 3 cm. When $U_{j\max} = 40$ cm/s, the generated eddies were clearly larger than the naturally occurring ones and extended outward to 5–6 cm. The streamwise scale of the generated eddies depended upon the amount of time the jet was emitting fluid during each cycle. The spacing between the eddies was proportional to the period of the jet. Although the acceleration and deceleration of the jet were varied, no obvious correlation was found between these parameters and the generated eddy structures.

Hot-film probes were used in the present investigation to record the instantaneous streamwise velocity components. Three such records are depicted in Fig. 6 for the natural and perturbed turbulent boundary layers at $x = 100$ cm. At $y/\delta = 0.6$, the natural boundary layer had a mean velocity of $0.9U_\infty$ and the typical random fluctuations are shown in the top record in the figure. When the probe was raised to $y/\delta = 0.8$, the mean velocity was increased to $0.96U_\infty$ and the negative spikes (marked by the arrows in the middle record) indicate the passing of natural, large-eddy structures by the fixed probe position. These eddies occur at random and have a mean frequency of approximately $0.13U_\infty/\delta$, as determined by visual examination of the velocity records. When secondary fluid was introduced from the spanwise slot at a period corre-

sponding to the mean natural period, the velocity records shown in the bottom of Fig. 6 result. Note that the hot-film probe was located 38 cm (16δ) downstream of the injection slot and the negative spikes resulting from the passing of the artificial eddies by the fixed probe are still periodic. Some differences exist, however, between the velocity signature of the natural eddies and the artificial ones. These differences depend upon the injection parameters which could possibly be further optimized to produce a more normal eddy structure.

The repeatability of the artificial structures was quite evident from the instantaneous streamwise velocity records. The negative spikes were always periodic but some slight changes in their amplitude were observed, due probably to their interactions with the random background turbulence. It was also noted that, when the boundary layer was perturbed, the artificially generated periodic structures dominated the flow and the naturally occurring random eddies were no longer observed visually or with the hot-film probe. This observation obviously depends upon the maximum amplitude of the jet perturbation. The smallest perturbation velocity tested was 20 cm/s. At this amplitude, the artificial eddies were more dominate than the natural eddy structures.

VI. Effects of Artificial Large-Scale Structures on Bursting

In the previous section, the similarity between the artificial (periodic) and the natural (random) structures has been established. An unexpected additional benefit of the large-eddy generating device was discovered during the present experiments; namely, the periodic large-eddy structures trigger the generation of bursting events near the wall of the flat plate. That is, not only the large eddies that characterize the outer parts of a turbulent boundary layer become periodic, but also the near-wall bursts, which randomly occur in a natural boundary layer, seem to be occurring more regularly.

A side view of a naturally occurring bursting event is shown in Fig. 7. The wall region at $x=80$–90 cm is visualized using fluorescent dye seeping from a spanwise slot just upstream of the observation station and the flow is from left to right. The time measured from an arbitrary origin is indicated underneath each photograph. The apparent accumulation of dye is caused by the formation of a low-speed region as observed by Kline et al.[11] and the lifting and breakup of this region is evident in the photographic sequence shown in the figure.

As shown by Gad-el-Hak and Hussain,[12] bursting events can also be induced artificially by withdrawing near-wall fluid from two minute holes separated in the spanwise direction or by pitching a miniature delta wing that is flush-mounted to the wall. Either of these two actions generates a hairpin-like vortex and low-speed streak that resemble naturally occurring structures. The resulting sequence of events that occur at a given location can then be uniquely controlled, thus allowing detailed examination via phase-locked measurements.

In contrast to the above method of inducing bursts by simulating wall events, in the present investigation the passing of an artificially induced, periodic large-eddy structure seems to trigger a bursting event near the wall. This is shown convincingly in the ciné films from which one example is depicted in Fig. 8 at $x=100$–110 cm. For this case, the maximum injection speed was 45 cm/s and the ball valve's temporal parameters were (0.1, 0.1, 0). It was evident from this and other cases that the passing of the artifically generated large-eddy structure triggered a burst-like event in the wall region. The ciné films showed that the bursting event was definitely phase locked with the large scale eddies and thus had a mean frequency corresponding to the imposed perturbation. Usually by the time a bursting event was clearly evident, as at $t=0.14$ s in Fig. 8, it appeared near the trailing edge of the large outer eddy. This observation seemed to be independent of the jet velocity and temporal parameters. Since only the centerline was studied, the spanwise structure of the above correlation is not clear.

The burst detection algorithm described in Sec. III F was used to establish the similarity between the artificially induced wall events and the naturally occurring ones. The burst detector searches for periods of high acceleration without necessarily larger fluctuations than the background turbulence. As shown by Blackwelder and Kaplan,[9] such periods are associated with events characterized by a high degree of coherence in time and correspond to eddies having a conditionally averaged Reynolds shear stress that is an order of magnitude greater than its conventionally averaged value. Whenever an artifically generated large-eddy structure passed the fixed velocity probe located very near the wall, a single burst was detected by the pattern-recognition algorithm; thus further confirming the visualization results depicted in Fig. 8.

VII. Spectral Analysis

The autocorrelation and spectrum of the longitudinal velocity fluctuations were used to analyze the intermittent signal from a hot-film probe located near the outer portion of a turbulent boundary layer and to determine the effects of the large-eddy generating device. The autocorrelation coefficient is the correlation between the values of the streamwise velocity fluctuations u at two different times nondimensionalized using

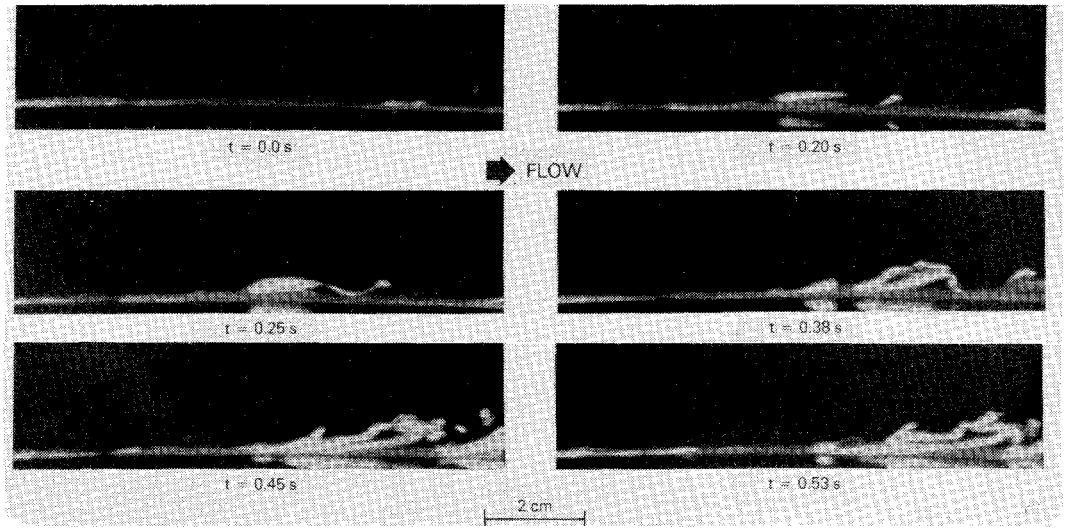

Fig. 7 Naturally occurring bursting event in a turbulent boundary layer.

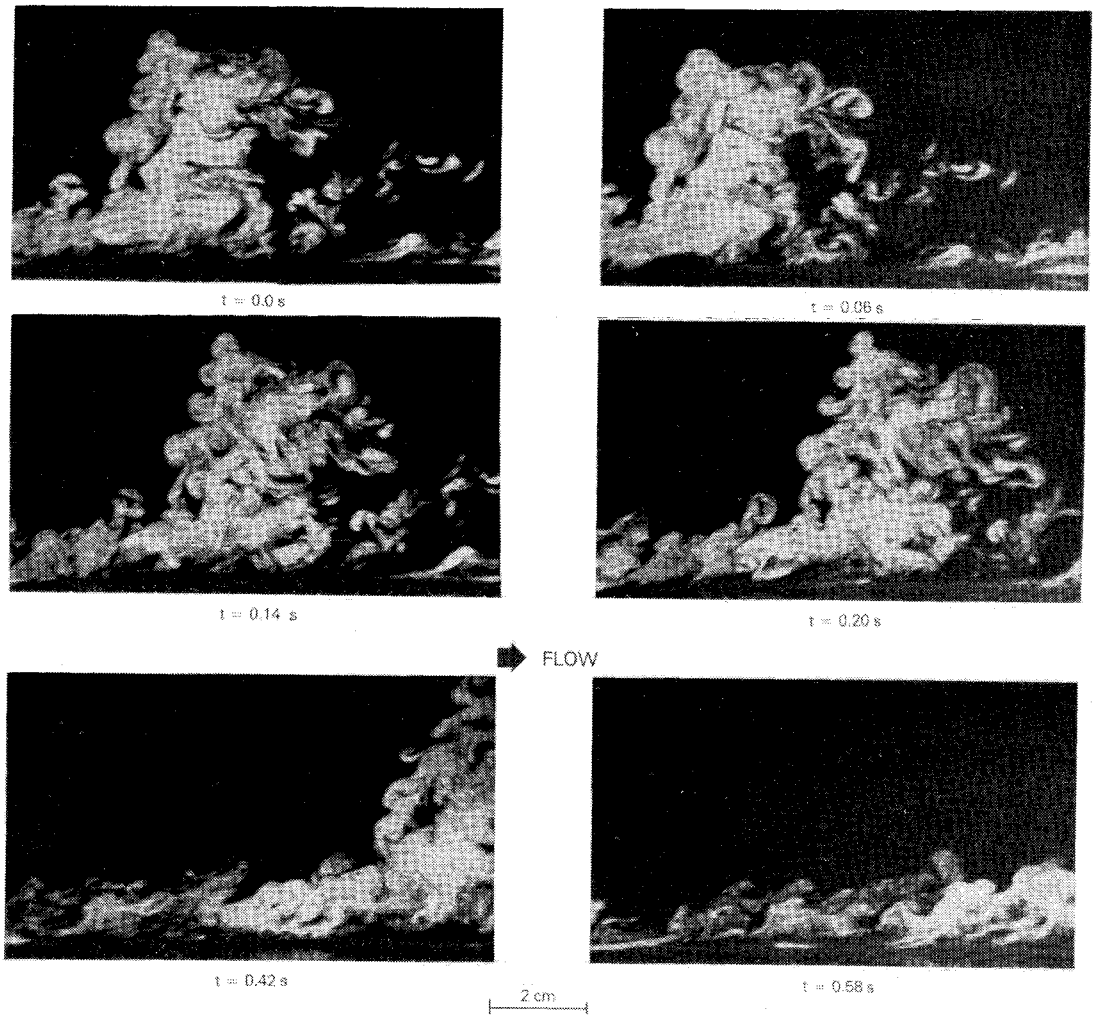

Fig. 8 A bursting event triggered by the passing of an artificial large-eddy structure.

the mean square:

$$R(\tau)=\overline{u(t)u(t-\tau)}/\overline{u^2}$$

where the overbar denotes a time average. The Fourier transform of the autocorrelation coefficient is the power spectral density:

$$S(f)=\frac{1}{2\pi}\int_{-\infty}^{\infty} e^{-2\pi\tau f}R(\tau)\mathrm{d}\tau$$

which is the normalized spectral distribution of the squared intensity of the longitudinal velocity fluctuations. These two functions provide a convenient method of determining length scales in the flowfield and may provide clues to periodic and/or other structures embedded in the random velocity fluctuations.

The effects of the large-eddy generating device on the dimensional spectral distribution $[S'(f)=\overline{u^2}S(f)]$ and the autocorrelation coefficient are elucidated by comparing these statistical quantities for a natural boundary layer and a perturbed one as shown in Fig. 9. In both cases, the ambient flow speed was $U_\infty=20$ cm/s and the probe was located at $x=67$ cm and $y/\delta=0.6$. For the perturbed case the maximum injection speed was 40 cm/s and the temporal parameters were (0.1, 0.4, 0). A pronounced spectral peak is evident in Fig. 9 at a frequency of 2 Hz. Also, a corresponding oscillation appears in the autocorrelation coefficient with a period of approximately 0.5 s corresponding to the period of the cyclic jet.

Other comparisons were made for other temporal parameters of the jet. When the ball valve opened more slowly with temporal parameters (1.0, 0.25, 0), the spectrum had a well-defined peak as in Fig. 9 and higher harmonics were observed in the spectrum. This is consistent with the strong asymmetry between the acceleration and deceleration times. The periodic structure of the autocorrelation function was also skewed positively; i.e., had sharp positive peaks and broad valleys.

As evident from comparing the area under the spectral distribution curves for the natural and perturbed boundary layers, the mean square of the streamwise velocity fluctuations is increased by the introduction of the cyclic secondary fluid into the turbulent boundary layer. However, as seen from Fig. 6, much of this increase is due to the larger negative excursions of the velocity and not due to an increase in the fluctuations at every phase of the cycle. That is, an examination of the fluctuations between the artificial spikes reveals that the turbulence level is no larger than in the natural case and appears to be more stationary.

VIII. Probability Distribution

In Fig. 10, comparison is made between the probability density function of the streamwise velocity fluctuations for the natural and the perturbed boundary layers. The abscissa is the streamwise velocity, and the ordinate is a probability density

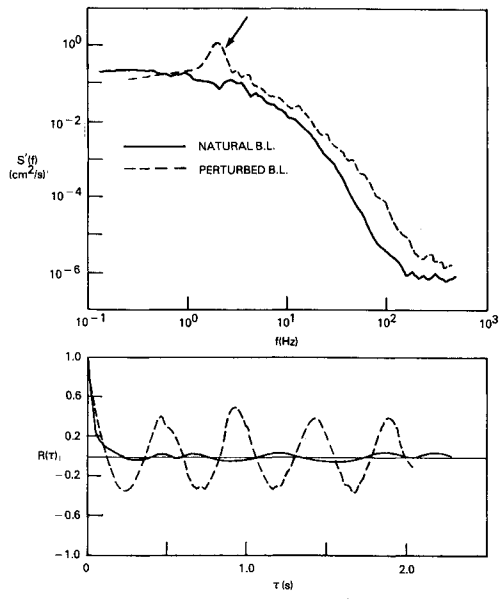

Fig. 9 Spectrum and autocorrelation for natural and perturbed boundary layers: $U_\infty = 20$ cm/s, $x = 67$ cm, $y/\delta = 0.6$.

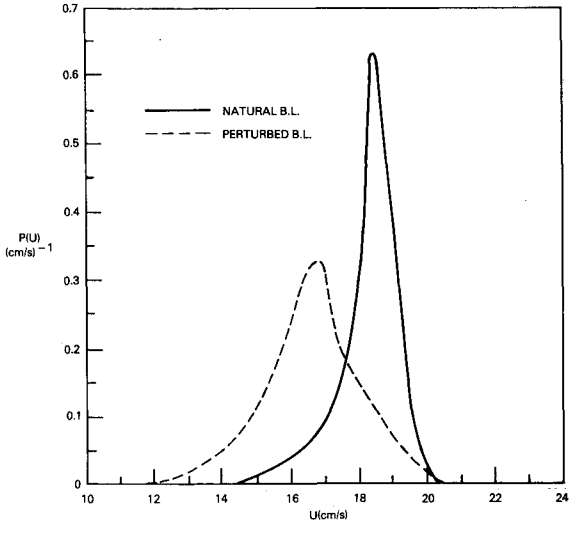

Fig. 10 Effects of periodic injection on probability density function: $U_\infty = 20$ cm/s, $x = 67$ cm, $y/\delta = 0.6$.

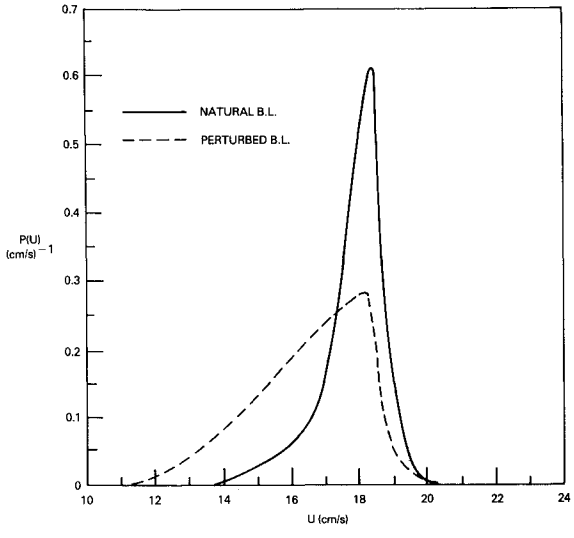

Fig. 11 Effects of periodic injection on probability density function: $U_\infty = 20$ cm/s, $x = 100$ cm, $y/\delta = 0.6$.

function normalized such that the area under the curve is unity. For both cases depicted in the figure, the hot-film probe was located at $x = 67$ cm and $y/\delta = 0.6$. The maximum injection speed was 40 cm/s and the temporal characteristics were (0.1, 0.4, 0). Both probability distributions are slightly skewed, i.e., the mean velocity is slightly lower than the most probable velocity. The distribution in the perturbed case is broader consistent with the higher turbulence levels.

The negative skewness of the perturbed case is more pronounced at $x = 100$ cm and $y/\delta = 0.6$, as shown in Fig. 11. The jet velocity was the same as the previous case and the temporal values were (1.0, 0.25, 0). At $y/\delta = 0.8$ under similar conditions, the turbulence level was lower and the probability distribution was narrower. Hence, it appears that the large-eddy generating device results in a broader, more negatively skewed probability distribution. Both these effects are a result of the higher turbulence levels generated by the cyclical injection and are consistent with the instantaneous velocity records depicted in Fig. 6.

IX. Summary

An active flow control device to generate large-scale, periodic structures in a turbulent boundary layer was explored in the present experimental investigation. Periodic large-eddy structures were artificially generated by cyclically injecting secondary fluid from a spanwise slot. A high degree of control of the cyclical injection was achieved by using a pressure regulator and a computer-driven ball valve. Within the limitations of the experimental apparatus, the maximum injection speed from the spanwise slot, the acceleration and deceleration rates of secondary fluid's injection, and the delay time between successive cycles were changed to optimize the simulation of large-eddy structures in a given turbulent boundary layer. The boundary-layer flow was visualized by fluorescent dyes injected either from the large-eddy generating device or from a second spanwise slot downstream. Important statistical quantities, such as the mean, the root mean square, the autocorrelation, the spectrum, and the probability distribution, were computed from the instantaneous velocity records of hot films to assess the effectiveness of the flow control device.

A range of large eddies could be generated depending upon the operating parameters. With a perturbation velocity of approximately U_∞ and frequency comparable to that of the naturally occurring eddies, large structures similar to the natural ones were produecd as seen in Fig. 4. However, when the jet velocity exceeded U_∞, larger eddies were generated. Figure 8 shows one example with $U_{j\max} \simeq 2U_\infty$. The simulated eddy extends beyond the nominal boundary layer and has a normal length scale of 2δ.

The negative velocity spikes, resulting from the passing of the artificial eddies by a fixed hot-film probe, were periodic and easily recognized at a distance 16δ downstream of the large-eddy generating device. However, some differences existed between the velocity signature of the natural and the artificial eddies. The temporal characteristics of the velocity spike depended upon the acceleration and deceleration of the jet suggesting that the injection parameters could be further optimized to produce a more naturally appearing spike. The artificially generated periodic structures dominated the flow, and the natural random eddies were no longer observed visually or with a hot-film probe. Lower excitation amplitudes should be studied to determine how the simulated and natural eddies interact.

At a given location in the boundary layer, the injection device resulted in slightly lower mean velocity but higher turbulence levels. However, much of the increase in the turbulence level is due to the larger negative excursions of the velocity and not due to an increase in the fluctuations at every phase of the cycle.

A dominant spectral peak and a corresponding oscillation in the autocorrelation coefficient appeared at the injection frequency. Higher harmonics could be observed in the spectral

distribution whenever the generation jet was strongly skewed in time. The probability distributions were more broad and more negatively skewed in the case of the perturbed boundary layer as compared to the distributions in a natural turbulent boundary layer.

In addition to removing the inherent randomness in large-eddy structures, the periodic large eddies generated from the spanwise slot seemed to trigger the generation of bursting events near the wall of the flat plate. These events were phase-locked with the large structures and appeared consistently near the trailing edge of the large eddies. Thus, both the large eddies and bursts occurred more regularly in the perturbed turbulent boundary layer, even at stations considerably downstream of the large-eddy generating device. In other words, the device considered in the present investigation is capable of producing periodic structures in both the outer and inner regions of a turbulent boundary layer.

There are, however, some important issues that remain to be addressed by future research. For example, the naturally occurring eddies are not two-dimensional, although no attempt was made in the present investigation to examine the third dimension of the simulated eddies. Similarly, the spanwise structure of the bursting events associated with the simulated eddies was not studied. The correlation between the large eddies and the bursting process is dependent upon the Reynolds number in natural boundary layers. Hence, some variation of the Reynolds number should be undertaken. Also an optimization of parameters and other methods to reduce the high turbulence levels introduced by the control device would be desirable.

Acknowledgments

This work is supported by the National Aeronautics and Space Administration-Langley Research Center under Contract NAS1-18213 and monitored by John C. Lin. The continuous support of Dennis M. Bushnell is greatly appreciated.

References

[1]Viets, H., "Coherent Structures in Time Dependent Shear Flows," *Turbulent Boundary Layers*, AGARD/NATO CPP-271, Nevilly Sur Seine, France, Paper 5, 1980.

[2]Viets, H., Ball, M., and Bougine, D., "Performance of Forced Unsteady Diffusers," AIAA Paper 81-0154, Jan. 1981.

[3]Bushnell, D. M., "Turbulent Drag Reduction for External Flows," AIAA Paper 83-0227, Jan. 1983.

[4]Anders, J. B. and Watson, R. D., "Airfoil Large-Eddy Breakup Devices for Turbulent Drag Reduction," AIAA Paper 85-0520, March 1985.

[5]Gad-el-Hak, M. and Blackwelder, R. F., "The Discrete Vortices from a Delta Wing," *AIAA Journal*, Vol. 23, June 1985, pp. 961-962.

[6]Gad-el-Hak, M. and Blackwelder, R. F., "Control of the Discrete Vortices from a Delta Wing," *AIAA Journal* to be published.

[7]Gad-el-Hak, M., Blackwelder, R. F., and Riley, J. J., "On the Growth of Turbulent Regions in Laminar Boundary Layers," *Journal of Fluid Mechanics*, Vol. 110, Sept. 1981, pp. 73-95.

[8]Kovasznay, L. S. G., Kibens, V., and Blackwelder, R. F., "Large-Scale Motion in the Intermittent Region of a Turbulent Boundary Layer," *Journal of Fluid Mechanics*, Vol. 41, April 1970, pp. 283-325.

[9]Blackwelder, R. F. and Kaplan, R. E., "On the Wall Structure of the Turbulent Boundary Layer," *Journal of Fluid Mechanics*, Vol. 76, July 1976, pp. 89-112.

[10]Purtell, L. P., Klebanoff, P. S., and Buckley, F. T., "Turbulent Boundary Layer at Low Reynolds Number," *Physics of Fluids*, Vol. 24, May 1981, pp. 802-811.

[11]Kline, S. J., Reynolds, W. C., Shraub, F. A., and Runstadler, P. W., "The Structure of Turbulent Boundary Layers," *Journal of Fluid Mechanics*, Vol. 30, Dec. 1967, pp. 741-773.

[12]Gad-el-Hak, M. and Hussain, A. K. M. F., "Coherent Structures in a Turbulent Boundary Layer. Part 1: Generation of 'Artificial' Bursts," *Physics of Fluids*, Vol. 29, July 1986, pp. 2124-2139.